Molecular Oxygen Dependent Steps in Fatty Acid Oxidation by Cyclooxygenase-1†

Arnab Mukherjee, David W. Brinkley, Keng-Ming Chang, and Justine P. Roth*

Department of Chemistry, Johns Hopkins University, 3400 North Charles Street, Baltimore, Maryland 21218

Received December 4, 2006; Revised Manuscript Received January 9, 2007

ABSTRACT: The mechanism by which cyclooxygenase-1 (COX-1), a heme- and tyrosyl radical-containing enzyme, catalyzes the regio- and stereospecific oxygenation of polyunsaturated fatty acids to prostaglandin or hydroperoxide products has not been understood. Steady-state kinetic studies conducted with the native substrate arachidonic acid and the slower substrate linoleic acid are described here. Second-order rate constants, k_{cat}/K_M for fatty acid and O_2, are found to depend upon the concentration of the other cosubstrate. Competitive oxygen kinetic isotope effects (^{18}O KIEs) $k_{cat}/K_M(^{16,16}O_2)/k_{cat}/K_M(^{18,16}O_2)$ reveal that a peroxyl radical is formed in or before the first kinetically irreversible step. Together, the results indicate that the oxygenase reaction occurs by a sequential mechanism which most likely involves reversible abstraction of a hydrogen atom from the fatty acid prior to the trapping of the delocalized substrate radical by O_2. The identity of the first kinetically irreversible step, subsequent to forming the peroxyl radical, is also discussed in the context of the magnitude of the oxygen kinetic isotope effects as well as the behavior of $k_{cat}/K_M(O_2)$ in response to changing solvent pH, pD, and viscosity.

Cyclooxygenases (COX-1 and COX-2)[1] are structurally homologous membrane proteins that use a heme prosthetic group and a tyrosyl radical to mediate the first committed step in prostanoid biosynthesis (*1*, *2*). COXs exhibit two activities (Scheme 1): (i) a dioxygenase activity where O_2 is regio- and stereospecifically incorporated into a fatty acid substrate and (ii) a peroxidase activity where two reducing equivalents are used to convert a hydroperoxide to an alcohol (*3*). Prostaglandin H_2, produced from arachidonic acid by the dioxygenase and peroxidase reactions of COX, is the precursor to all other prostaglandins in addition to thromboxane and prostacyclin. Pathways leading to the formation of prostanoids which are independent of COX may also exist (*4*). Collectively, these substances mediate a range of physiological processes from cell differentiation and proliferation to inflammation and oxidative stress (*1*−*8*). Understanding the reactivity of COX with molecular oxygen is relevant to the enzyme's potential involvement in certain diseases (*9*, *10*) as well as the mechanism by which prostaglandin is formed in preference to acyclic hydroperoxyeicosatetraenoic acids (*1*).

COX-1 was one of the first enzymes proposed to use an amino acid radical for catalysis (*11*−*13*). Tyrosyl radicals have since been identified in both COX isoforms (*14*) and shown to originate from a hydroperoxide-dependent process which involves oxidation of a noncovalent, enzyme-bound ferric protoporphyrin IX {Fe^{III}Por} to a highly reactive ferryl species {Fe^{IV}(O)$Por^{•+}$}. Decay of Fe^{IV}(O)$Por^{•+}$ to Fe^{IV}(O)Por occurs on the millisecond time scale at rates that correlate with the appearance of an EPR signal assigned to Tyr385• (*15*−*20*). Tyr385 is located ∼9 Å from the closest meso position of the porphyrin ring at the top of the hydrophobic substrate-binding domain (Figure 1).

Scheme 1

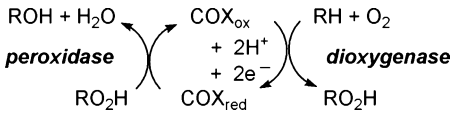

The detailed mechanism of site-specific tyrosine activation in COX has not been understood. This reaction requires the selective removal of an electron from Tyr385 in spite of other oxidizable residues (Tyr348 and Trp387) within a similar distance of the Fe^{IV}(O)$Por^{•+}$. Radical equivalents at other tyrosines in COX have been detected and are thought to arise from the initially formed Tyr385• (*22*, *23*). Tyrosyl radical-forming reactions have also been reported in a variety of metalloenzymes (*24*) including structurally and functionally disparate heme proteins (*25*−*29*). The reaction in COX appears unique, however, in that the Tyr385• initiates C−H oxidation and is catalytically regenerated through a series of reactions which involve O_2. Similar mechanisms have been considered in plant-derived fatty acid oxygenases which appear to require heme and a specific tyrosine residue for catalysis (*30*−*33*).

Crystal structures of COX-1 (*21*) reveal that arachidonic acid binds ∼12 Å from the heme in a distorted L-shaped conformation which positions the 13-*pro-S* hydrogen for abstraction by Tyr385• (Figure 2). A similar more extended binding conformation is indicated for the substrate analogue linoleic acid (*34*), which has two fewer carbons and two fewer double bonds. This conformation causes the bisallylic 11-*pro-S* hydrogen to point toward the oxygen of Tyr385•.

† Funding was provided by grants from the ACS-PRF (40731-G3), NSF CAREER (CHE-0449900), and the Research Corporation Cottrell Scholar Award (CS-1461) to J.P.R.

* Corresponding author. Phone: 410-516-7835. Fax: 410-516-8420. E-mail: jproth@jhu.edu.

[1] Abbreviations: COX-1, cyclooxygenase isoform-1; COX-2, cyclooxygenase isoform-2; LOX-1, soybean lipoxygenase; ^{18}O KIE, oxygen-18 kinetic isotope effect; ^{18}O EIE, oxygen-18 equilibrium isotope effect.

10.1021/bi602502j CCC: $37.00
Published on Web 03/14/2007

While the structures of the enzyme-bound arachidonate and linoleate complexes are consistent with the regio- and stereospecific H• abstraction reactions demonstrated through isotope-labeling studies (*35*, *36*), these static snapshots provide little insight concerning how the enzyme directs the reactivity of the small, nonpolar, and freely diffusible substrate O_2.

To better understand how amino acid radicals catalyze selective oxygenations, we have investigated the reactions of COX-1 with arachidonic acid (AA) and the slower substrate analogue linoleic acid (LA). Previous studies have shown that 2 equiv of O_2 are incorporated during the dioxygenase reaction of AA, and PGG_2 is the main product (95%) along with small amounts of 11*R*, 15*S*, and 15*R* hydroperoxyeicosatetraenoic acids (HpETEs) (eq 1) (*37*, *38*).

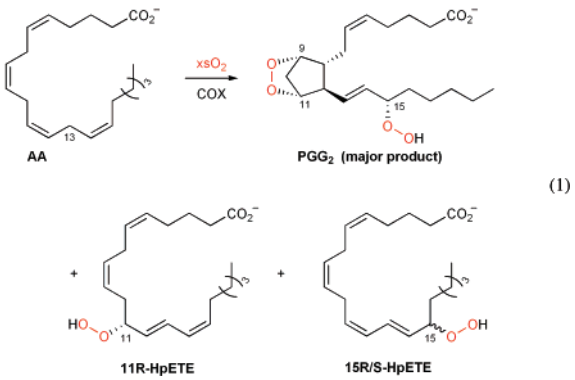

(1)

In a less selective dioxygenase reaction, which consumes only 1 equiv of O_2, LA is converted to 9(*R*)-hydroperoxy-octadecadienoic acid (HpOD) (~70%) in addition to the 9*S*, 13*R*, and 13*S* isomers (eq 2) (*39*). In the following studies,

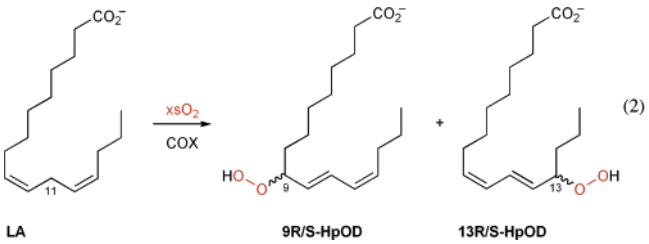

(2)

steady-state kinetics as a function of pH, solvent isotope, and solvent viscosity as well as competitive oxygen kinetic isotope effects are employed to provide detailed insights concerning the O_2-dependent transformations in the reactions mediated by COX-1.

MATERIALS AND METHODS

General. All chemicals were obtained commercially in the highest purity available. Arachidonic acid [5(*Z*),8(*Z*),11(*Z*),-14(*Z*)-eicosatetraenoic acid] and flurbiprofen were supplied by Sigma. Linoleic acid [9(*Z*),12(*Z*)-octadecadienoic acid] was supplied by Acros. Prostaglandin H_2 [15(*S*)-hydroxy-9,11-peroxidoprosta-5(*Z*),13(*E*)-dienoic acid (PGH_2)], prostaglandin G_2 [15(*S*)-hydroperoxy-9,11-peroxidoprosta-5(*Z*),13(*E*)-dienoic acid (PGG_2)], 15(*S*)-hydroperoxy-5(*Z*),8-(*Z*),11(*Z*),13(*E*)-eicosatetraenoic acid (15*S*-HpETE), 9(*R*)-hydroperoxy-10(*E*),12(*Z*)-octadecadienoic acid (9*R*-HpOD), and 13(*S*)-hydroperoxy-9(*Z*),11(*E*)-octadecadienoic acid (13*S*-HpOD) were supplied by Cayman Chemicals as ethanolic

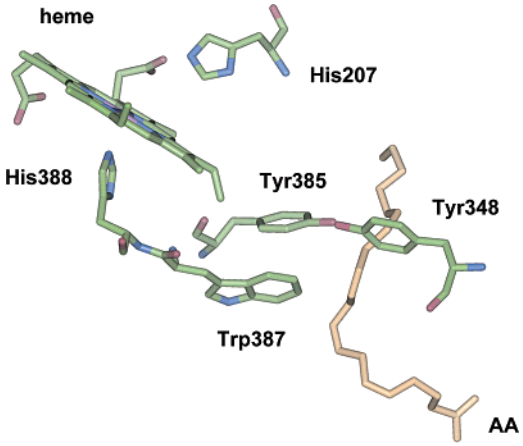

FIGURE 1: Disposition of the peroxidase and dioxygenase active sites in COX-1. The crystal structure (1DIY) was obtained with Co^{III}-protoporphyrin IX in place of the heme (*21*).

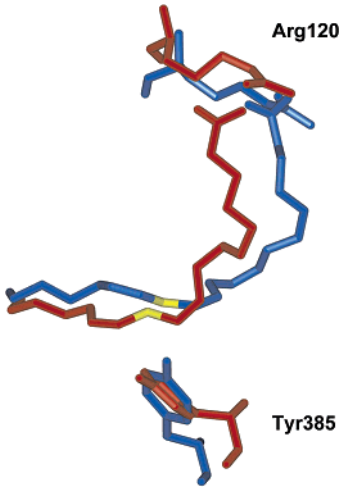

FIGURE 2: Superimposed structures of linoleate (red, 1IGZ) (*34*) and arachidonate (blue, 1DIY) (*21*) bound to COX-1 with the C-11 and C-13 positions of the respective fatty acids designated (yellow).

solutions. Substrate stock solutions were prepared inside an anaerobic glovebox (MBraun) by dissolving the neat fatty acid in deoxygenated buffer. Aliquots were stored at −30 °C under N_2 and thawed just before use.

Enzyme Preparation. COX-1 was isolated from ram seminal vesicles (Oxford Biomedical) following the procedure of Marnett et al. (*40*). Purity was estimated to be >95% by gel electrophoresis. Approximately 60% of the isolated protein contained the heme prosthetic group as judged from the Soret band absorbance of Fe^{III}Por ($\epsilon_{412nm} = 123000\ M^{-1}\ cm^{-1}$) (*41*) and the total protein content estimated by Bradford analysis. As reported previously, preparations containing the apoprotein (~40%) could be reconstituted with hematin (Sigma), and significant dioxygenase activity was recovered (*42*).

The concentration of holoprotein determined from the Soret absorbance at 412 nm using a diode array spectrophotometer (Agilent HP 8453) was correlated to the enzyme activity for six different preparations of COX-1. Enzyme activity was determined using a Clark-type oxygen electrode (Yellow Springs Inc.; 5300A voltmeter and 5331A probe). Rates of O_2 consumption were confirmed to be due to COX activity based on the inhibition patterns observed upon adding flurbiprofen (*43*, *44*). A standard assay was developed using

solutions of holoprotein that did not contain added hematin. It was assumed that each equivalent of Fe^{III}Por gave rise to 1 equiv of active enzyme. The actual concentration of active enzyme may be somewhat lower in view of results from rapid freeze−quench electron paramagnetic resonance (EPR) studies which indicate that the ratio of the catalytic tyrosyl radical to heme is ~0.6 for COX-1 (*20*). The EPR experiments are not directly comparable, however, since they were conducted at 10^3-fold higher concentrations of enzyme and without added substrate.

Steady-State Kinetics. Initial rate measurements were performed using the O_2 electrode as described below. Reaction temperatures were maintained at 30 ± 0.2 °C using a recirculating water bath (VWR 116-0S). In addition to the fatty acid and O_2, solutions contained 1 mM phenol and 1 μM hematin unless noted otherwise. The phenol is a peroxidase substrate which prevents enzyme deactivation due to the accumulation of hydroperoxide products under turnover conditions. As described in the following section, experiments at varying phenol concentrations were performed to expose any dependence of the dioxygenase reaction kinetics upon the peroxidase reaction (*45*, *46*). Trace diethyldithiocarbamate (DDC) used as a stabilizer during protein isolation was also present in the kinetic assays. Addition of DDC was confirmed to have no effect upon the dioxygenase kinetics, consistent with previous reports (*47*).

Kinetics experiments were conducted at 30 °C at pH 8 (0.016 M sodium pyrophosphate, $\mu = 0.1$ M) unless noted otherwise. Reactions were initiated by adding between 0.5 and 5 μL of an enzyme stock solution to 1 mL of a rapidly stirring solution containing the dioxygenase and peroxidase substrates. This solution was preequilibrated against air or a mixture of pure O_2 and N_2 at 1 atm. Standard assays in air-saturated solutions containing either 30 μM AA or 50 μM LA were performed to check the activity of the enzyme. The enzyme concentrations were standardized from the rates using the rate constants $v/[E]_T = 124\ s^{-1}$ for AA and $v/[E]_T = 12.8\ s^{-1}$ for LA. The latter values agree well with specific activities for ovine COX-1 reported in the literature (*48*).

The concentration of active COX-1 was typically 1.0−3.0 nM in experiments with AA and 5.0−20 nM in the experiments with LA. The addition of hydroperoxide compounds to initiate enzyme activity was unnecessary in the experiments performed due to the trace levels present as impurities in the fatty acid substrate solutions (*48*). No lag in the rate of O_2 uptake was detectable in any of the experiments even at the lowest concentrations of fatty acids examined (2 μM AA and 6 μM LA). Furthermore, the kinetic parameters were found to be unaffected by addition of 15*S*-HpETE, 13*S*-HpOD, and 9*R*-HpOD as described in Results.

Rates of O_2 consumption varied, as expected, in direct proportion to the concentration of COX-1. Control experiments were especially important here since artifacts due to electrode dampening and inadequate mixing have been reported with AA at enzyme concentrations >10 nM (*49*, *50*). COX-1 loses much of its activity within 20−60 s depending on the reaction conditions. Initial rates were, therefore, calculated from the most linear portion of the decay curve 5 s after introduction of the enzyme to allow for mixing. Rates ranged from 4×10^{-8} M s^{-1} to 4×10^{-7} M s^{-1}, and small corrections were applied for the background drift of the oxygen electrode. The drift rate was less than 30% of the enzymatic rate in any given experiment.

Analysis of the Initial Rate Data. The initial rate data were analyzed using Kaleidagraph 4.0 (Synergy Software). Kinetic parameters were obtained by fitting at least 10 points to the Michaelis−Menten expression:

$$\frac{v}{[E]_T} = \frac{{}^{ap}k_{cat}[S]}{{}^{ap}K_M + [S]} \tag{3}$$

where v is the initial rate, $[E]_t$ is the total active enzyme concentration, ${}^{ap}K_M$ is the apparent Michaelis constant, and ${}^{ap}k_{cat}$ is the apparent rate constant for enzyme turnover. The resulting k_{cat}, K_M, and k_{cat}/K_M are reported with ±1 standard errors accompanying the nonlinear regression analysis. Double reciprocal plots of $(v/[E])^{-1}$ vs [fatty acid]$^{-1}$ or $(v/[E])^{-1}$ vs $[O_2]^{-1}$ gave kinetic parameters with larger uncertainties, yet all were within the error of those derived from the nonlinear curve-fitting analysis.

pH and pD Profiles. The following buffers were used: 0.0566 M sodium phosphate at pH 7, 0.0160 M sodium pyrophosphate at pH 8, 0.0136 M sodium pyrophosphate at pH 9, 0.0107 M sodium pyrophosphate at pH 10, and 0.0200 M CAPS at pH 11. The ionic strength was $\mu \cong 0.1$ M in all cases. Deuterated buffer solutions were prepared similarly using salts which had been enriched by dissolution in D_2O (99.9% Cambridge Isotope Laboratories) and evaporation to dryness. Solution pH and pD values ($pD = pH_{reading} + 0.4$) were determined using an Accumet Research pH meter at 22 °C. Small corrections of −0.0028 unit/°C (phosphate), 0.01 unit/°C (pyrophosphate), and −0.018 unit/°C (CAPS) were applied to extrapolate to 30 °C. Solvent isotope effects are reported as the average of three measurements with the errors propagated according to the equation:

$$\Delta\left(\frac{k_{H_2O}}{k_{D_2O}}\right) = \sqrt{\left(\frac{1}{k_{D_2O}}\right)^2(\Delta k_{H_2O})^2 + \left[\frac{-k_{H_2O}}{(k_{D_2O})^2}\right](\Delta k_{D_2O})^2} \tag{4}$$

where $k_{H_2O} = [k_{cat}/K_M(O_2)]_{H_2O}$, $k_{D_2O} = [k_{cat}/K_M(O_2)_{D_2O}]$, and Δk corresponds to the standard error from the nonlinear regression analysis.

Viscosity Effects. Experiments to probe the effects of solution viscosity upon $k_{cat}/K_M(O_2)$ and k_{cat}/K_M(fatty acid) were conducted using sucrose as the viscosogen. Viscosities were determined relative to a solution containing only buffer using an Ostwald viscometer at 30 °C. The resulting data were fitted to $[k_{cat}/K_M(O_2)]^0/[k_{cat}/K_M(O_2)] = (\eta/\eta^0)^{exp}$, where the superscript 0 designates the absence of added viscosogen. According to the Stokes−Einstein relation, an exponent of 1 is expected for diffusion-limited binding of the fatty acid substrate or the dissociation of the hydroperoxide product (*51*). A smaller, empirically determined exponent of 0.5 has been proposed to describe the deviations from Stokes−Einstein behavior for small diatomic solutes like O_2 (*52*, *53*).

Competitive Oxygen Kinetic Isotope Effects. A previously described technique (*54*) employing natural abundance O_2 and isotope ratio mass spectrometry (IRMS) was used to determine competitive oxygen kinetic isotope effects (^{18}O KIEs). The general procedure involves isolating O_2 from

solutions and analyzing its $^{18}O/^{16}O$ before and after an enzymatic reaction has taken place.

Experiments were conducted at 23 ± 2 °C in Tris−sulfate buffer (50 mM, pH 8, $\mu = 0.1$ M) or pyrophosphate buffer. Substrate-containing solutions were saturated with O_2/He gas mixtures, loaded into a collapsible and injectable Tedlar bag (Midan Co.) and connected to the vacuum apparatus. Fixed volumes of solution were withdrawn from the reaction vessel to isolate the O_2 for analysis. Enzymatic reactions were initiated by injecting a COX-1 solution through a resealable septum. Fixed volumes of the reaction solution were again removed, and the enzymatic reaction was quenched by addition to 5-sulfosalicylic acid in 85% H_3PO_4. The fractional consumption of O_2 was determined to ±3% using a capacitance manometer (Omega PX238). No O_2 was consumed when the enzyme was introduced into solutions containing an excess of the inhibitor flurbiprofen (30 μM) (*43*, *44*). Samples of O_2 were purified from other condensable gases, quantitatively converted to CO_2, and condensed into dry glass tubes which were then flame-sealed (*54*).

The CO_2 samples were analyzed using dual inlet stable isotope mass spectrometers housed in the Water Sciences Laboratory at the University of Nebraska (Lincoln, NE) and the Environmental Isotope Laboratory at the University of Waterloo (Ontario, Canada). The $^{18}O/^{16}O$ in samples prepared using the above outlined procedure was precise to ±0.0003. The isotope fractionation of the unreacted O_2 was interpreted using the equation

$$^{18}\text{O KIE} = \left[1 + \frac{\ln(R_f/R_0)}{\ln(1-f)}\right]^{-1} \quad (5)$$

which expresses the ^{18}O KIE in terms of a ratio of ratios, i.e., the $^{18}O/^{16}O$ (R_f) at a specific fractional conversion (f) relative to the $^{18}O/^{16}O$ (R_0) prior to the enzymatic reaction. The ^{18}O KIEs reported in this work were determined at fractional conversions from ca. 5% to 65% by numerically solving eq 5. Each KIE is quoted as the average of at least 10 independent measurements with errors of ±1 SD about the mean.

Mass Spectral Analysis of Deuterium Exchange. The isotope composition of the fatty acid substrates was analyzed by electrospray ionization mass spectrometry (ESI-MS) using an LCQ Deca instrument (Thermo-Finnigan) equipped with an ion-trap analyzer and operating in negative ion mode. Samples were delivered at a rate of 10 μL/min directly onto a silica-fused capillary. The capillary voltage was 5 keV, and the desolvation temperature was 350 °C. Each spectrum spanning a mass-to-charge (m/z) ratio range of 50−500 was obtained by averaging 30 scans/min.

Incorporation of deuterium from D_2O into the substrate was examined for the enzyme reactions under turnover conditions. Ammonium acetate (10 mM, pD 7.6) was used as the buffer to minimize the manipulation of solutions prior to analysis. The kinetic parameters in this buffer were found to be similar to those in pyrophosphate (data not shown). Phenol and hematin were left out of the reaction solutions to prevent high conversions of the substrate to products. Experiments were performed by incubating the fatty acid (30−100 μM) with nanomolar concentrations of COX-1 and quenching after 10−20 s by addition of concentrated ammonium hydroxide to bring the pH to 12. The quenched reaction mixture was diluted 2-fold by addition of methanol and the protein removed by centrifugation at 14000 rpm through a Microcon 10 kDa spin column (Amicon) prior to MS analysis.

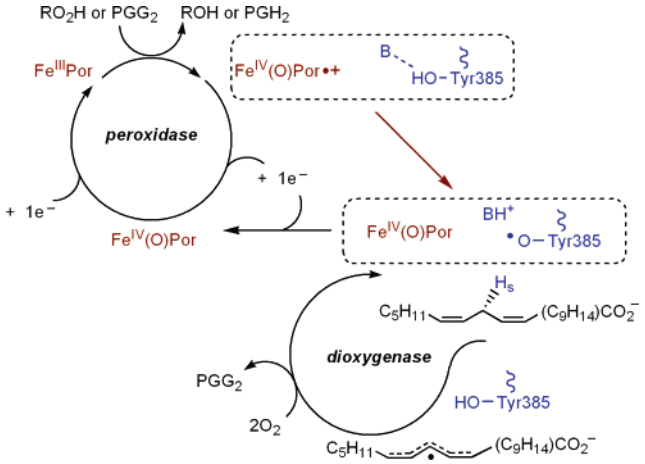

FIGURE 3: Branched-chain mechanism for the oxidation of arachidonic acid by COX.

RESULTS

The currently accepted model for COX reactivity involves a "branched-chain mechanism" with two separately functioning peroxidase and dioxygenase active sites (*1*, *55*−*57*). As shown in Figure 3, reactions of hydroperoxide compounds give rise to $Fe^{IV}(O)Por^{\bullet+}$. The ferryl species produces the catalytic tyrosyl radical (Tyr385$^\bullet$) by a long-range oxidation reaction which involves the removal of an electron together with a proton. The Tyr385$^\bullet$ then initiates oxygenation of the fatty acid substrate (*1*). The formation of Tyr385$^\bullet$ occurs in competition with the oxidation of exogenous reductants, such as phenol, by the $Fe^{IV}(O)Por^{\bullet+}$. While inhibitory at high concentrations, phenol present at lower concentrations protects the enzyme from overoxidation by the hydroperoxide products and, therefore, is commonly used in enzyme assays.

The branched-chain mechanism is consistent with a number of experimental results (*1*) including the requirement for hydroperoxide compounds to initiate dioxygenase catalysis (*58*, *59*) and the observation that dioxygenase activity may be unaltered in site mutants where the peroxidase reaction is significantly impaired (*55*). Trace hydroperoxide impurities present in the fatty acid preparations are usually sufficient to generate fully active enzyme in turnover experiments; this is because of the rapid formation of hydroperoxide products by the dioxygenase reaction in the pre-steady-state (*60*). In the present study, experiments were conducted under conditions where the steady-state level of the active enzyme containing Tyr385$^\bullet$ appears to be constant. This is a key feature which allows the kinetics of dioxygenase catalysis to be examined independently of the kinetics of the peroxidase reaction.

Steady-State Kinetics. COX reacts with a variety of C-18 and C-20 fatty acids that contain bisallylic C−H bonds (*48*, *61*−*64*). The following experiments compare the enzymatic oxygenation of the native substrate AA to that of the slower reacting analogue LA. The dependence of initial rates upon O_2 concentration is shown in Figure 4 for the two fatty acids at near-saturating concentrations ($\geq 6K_M$). The data, which appear to be reasonably well fitted by the Michaelis−Menten

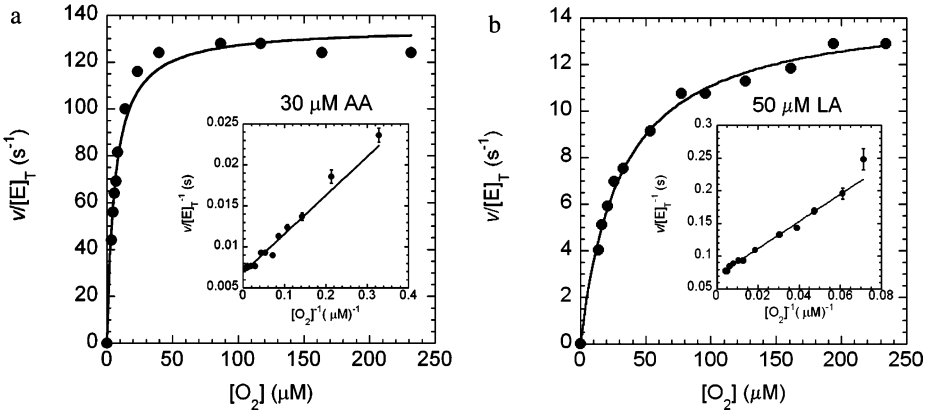

FIGURE 4: O_2 dependence of the initial rates of arachidonic acid (AA) and linoleic acid (LA) oxidation.

Table 1: Limiting Steady-State Kinetic Parameters for the Dioxygenase Reactions of COX-1

	k_{cat}[a] (s^{-1})	$k_{cat}/K_M(O_2) \times 10^{-6}$ ($M^{-1}\,s^{-1}$)	$K_M(O_2)$ (μM^{-1})	k_{cat}/K_M(fatty acid) $\times 10^{-6}$ ($M^{-1}\,s^{-1}$)	K_M(fatty acid) (μM^{-1})
AA	147 ± 6[b]	18.9 ± 0.9[b]	5.5 ± 0.8	46 ± 3[b]	1.9 ± 0.2
LA	17.7 ± 1.1	0.56 ± 0.02	24 ± 3	2.3 ± 0.2	8.2 ± 1.6

[a] Reported as the average results from independent experiments at varying concentrations of O_2 and fatty acid. [b] Not corrected for the stoichiometry of O_2 consumption.

equation, indicate the following parameters: $k_{cat} = 135 \pm 3$ s^{-1}, $K_M(O_2) = 5.9 \pm 0.5$ μM (*65*), and $k_{cat}/K_M(O_2) = (2.3 \pm 0.2) \times 10^7$ M^{-1} s^{-1} at 30 μM AA and $k_{cat} = 14.5 \pm 0.3$ s^{-1}, $K_M(O_2) = 31 \pm 2$ μM, and $k_{cat}/K_M(O_2) = (4.7 \pm 0.3) \times 10^5$ M^{-1} s^{-1} at 50 μM LA. Double reciprocal plots (shown as insets in Figure 4) with weighting give the same kinetic parameters within the experimental error limits. Correcting for the factor of 2 in O_2-to-fatty acid stoichiometry reveals that $k_{cat}/K_M(O_2)$ for AA is approximately 20 times greater than $k_{cat}/K_M(O_2)$ for LA. The reason for the sensitivity of $k_{cat}/K_M(O_2)$ to the fatty acid substrate is explored in the sections which follow. As a starting point, the apparent kinetic parameters are examined at varying substrate concentrations. The results are summarized in Table 1 and discussed in terms of the kinetic mechanism.

(A) Linoleic Acid. Kinetic measurements with LA reveal a hyperbolic increase in the apparent k_{cat} as well as the apparent k_{cat}/K_M(LA) when the O_2 concentration is varied (Figure 5a,b). The latter behavior is not significantly affected by reducing the concentration of phenol from 1.0 to 0.3 mM or by adding hydroperoxide initiators, such as 13*S*-HpOD, up to 5 μM (see Supporting Information). At both lower and higher concentrations of phenol, k_{cat}/K_M(LA) declines, signaling a decrease in the steady-state concentration of Tyr385$^\bullet$ (data not shown); these results would be expected for enzyme deactivation due to inefficient scavenging of the hydroperoxide product and inhibition of Tyr385$^\bullet$ formation, respectively.

Hyperbolic trends are also observed for the apparent k_{cat} and $k_{cat}/K_M(O_2)$ in response to increasing the concentration of LA from subsaturating to saturating levels (Figure 5c,d). Again, the apparent $k_{cat}/K_M(O_2)$ is not significantly perturbed upon varying the concentration of phenol between 0.3 and 1.0 mM or upon adding hydroperoxide compounds up to 5 μM (Figure 6).

The observations that the apparent k_{cat}/K_M(LA) values depend upon the concentration of O_2 and the apparent $k_{cat}/K_M(O_2)$ values depend on the concentration of LA have implications for the kinetic mechanism (see below). While similar results could arise from a decrease in the steady-state level of Tyr385$^\bullet$, no such evidence is indicated by the control experiments at varying concentrations of the peroxidase substrates (phenol and 13*S*-HpOD). In positive control experiments at lower phenol concentrations, the decay of the active enzyme is detectable, however, and results from effects upon k_{cat} and $K_M(O_2)$ (see Supporting Information). In addition, the absence of a measurable effect upon k_{cat}/K_M(LA) due to added hydroperoxide initiator is a particularly important result which argues against dissociation of the substrate radical from the enzyme active site at low concentrations of O_2. This event would lead to enzyme deactivation during turnover and thus give rise to an apparent effect upon k_{cat}/K_M(LA). In addition, no evidence has been reported in studies of COX-1 deactivation with the native and slow substrates which could be construed as consistent with loss of the substrate-derived radical from the enzyme active site (*66*).

(B) Arachidonic Acid. The very low K_M values associated with the oxidation of AA require the measurement of rates at very low substrate concentrations, some of which approach the detection limit of the O_2 electrode. In addition, $v/[E]_T$ versus [AA] plots exhibit a sigmoidal shape at fatty acid concentrations less than 2 μM. This behavior has been reported for COX-1 but not COX-2 and previously suggested to arise from allosteric binding of the substrate (*67*). More recently, the sigmoidicity has been attributed to incomplete feedback activation by the hydroperoxide product (*68*), consistent with the different levels of PGG_2 required to activate COX-1 (20 nM) and COX-2 (2 nM) (*57*). In the present studies, only data collected at concentrations of AA $\geq$ 2 μM were analyzed to avoid ambiguities in interpreting the steady-state kinetic mechanism.

Analogous to the results with LA, the apparent k_{cat} and k_{cat}/K_M(AA) increase hyperbolically in response to increasing the concentration of O_2 (Figure 7a,b). Yet, in contrast to the observations with the slower substrate, a change in the

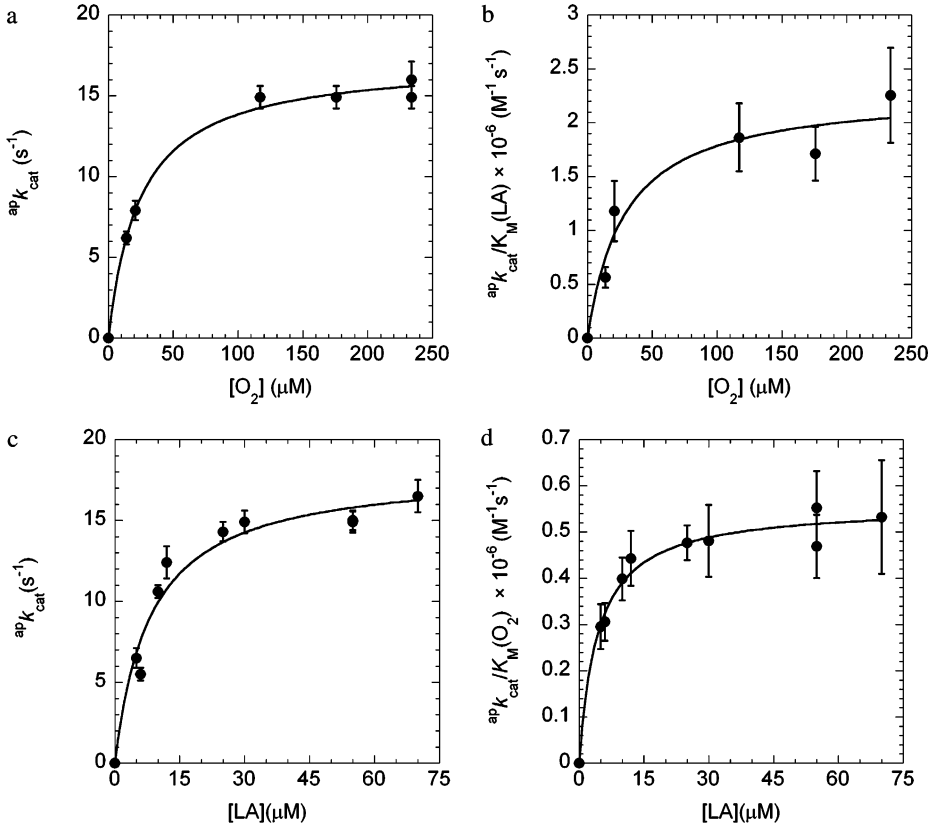

FIGURE 5: Effect of substrate concentration upon k_{cat} (a, c), k_{cat}/K_M(LA) (b), and $k_{cat}/K_M(O_2)$ (d).

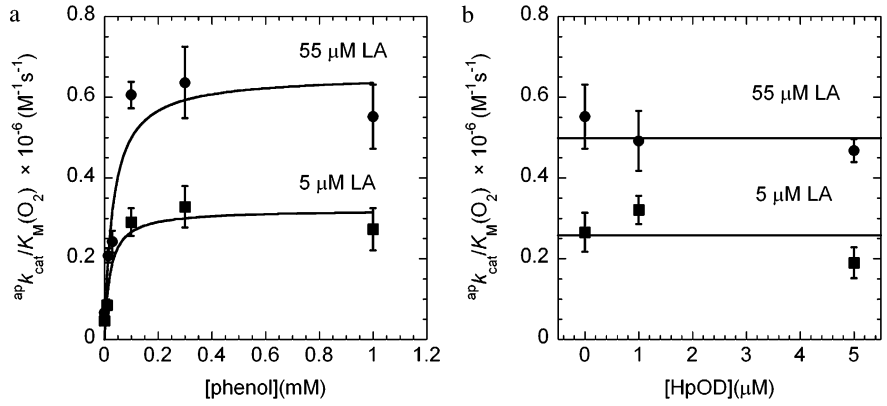

FIGURE 6: Apparent $k_{cat}/K_M(O_2)$ at varying concentrations of phenol (a) and 13-HpOD (b) and two different fixed concentrations of LA.

limiting $k_{cat}/K_M(O_2)$ is undetectable at the lowest concentration of AA examined (Figure 7d). This behavior is the result of a decrease in the $^{ap}k_{cat}$ and a commensurate decrease in the $^{ap}K_M(O_2)$ as the AA concentration is lowered. There is no discernible effect upon the steady-state level of Tyr385• at varying concentrations of the peroxidase substrates, i.e., from 0.3 to 1.0 mM phenol (*45*), and at varying concentrations of hydroperoxide initiator (9R-HpOD, 13*S*-HpOD, and 15*S*-HpETE) from 0.3 to 10 μM (see Supporting Information). At higher and lower concentrations of phenol, however, the k_{cat}/K_M(AA) and $k_{cat}/K_M(O_2)$ decrease, resembling the results obtained with LA.

Probing Diffusion-Limited Steps. Studies of k_{cat}/K_M(fatty acid) and $k_{cat}/K_M(O_2)$ as a function of solution viscosity were undertaken to expose possible contributions from diffusion-controlled steps. The results are shown in Figure 8 along with the expected theoretical behavior for a fully diffusion-limited process. Experiments at air saturation indicate that k_{cat}/K_M(AA) decreases slightly as the relative solution viscosity is increased whereas k_{cat}/K_M(LA) remains unchanged. Linear regression indicates slopes of 0.11 ± 0.03 and −0.034 ± 0.05, respectively. The very small viscosity dependence observed for AA originates from a decrease in k_{cat}. With the slower substrate, neither k_{cat} nor K_M(LA) is affected. These latter experiments serve as controls and indicate that the added viscosogen does not influence the kinetics by altering the protein's structure or stability (*51*). Similarly, no viscosity effect is discernible upon $k_{cat}/K_M(O_2)$ when LA is present at near-saturating concentrations. The analogous experiments with AA again indicate a slight diminution in $k_{cat}/K_M(O_2)$ due predominantly to an effect upon k_{cat}. Linear regression gives slopes of 0.14 ± 0.04 (AA) and 0.018 ± 0.013 (LA), well below expectations for a diffusion-limited reaction. The slopes in the two experiments performed with AA are consistent with a common unimolecular step limiting both k_{cat}/K_M(AA) and $k_{cat}/K_M(O_2)$.

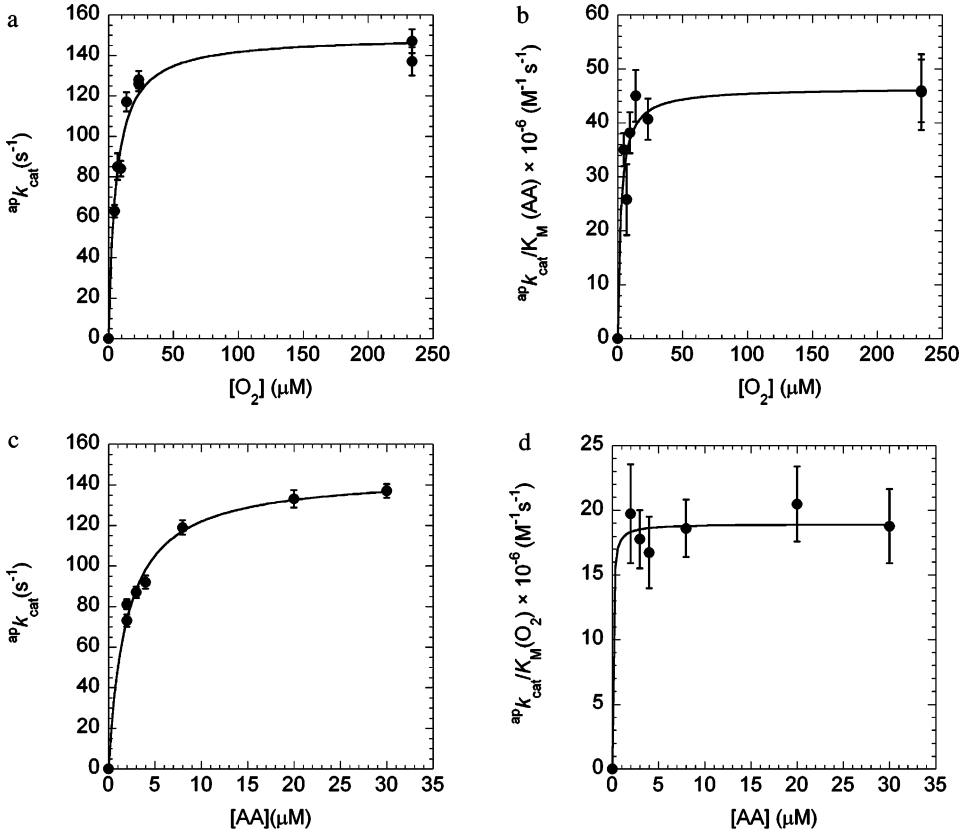

FIGURE 7: Effect of substrate concentration upon k_{cat} (a, c), k_{cat}/K_M(AA) (b), and $k_{cat}/K_M(O_2)$ (d).

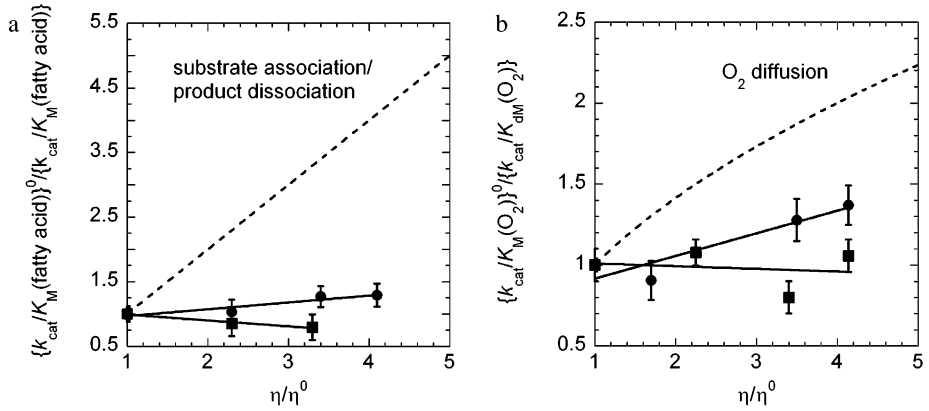

FIGURE 8: Effect of solution viscosity upon k_{cat}/K_M(fatty acid) (a) and $k_{cat}/K_M(O_2)$ (b) with AA (●) and LA (■). The dashed line is the theoretical relationship for a diffusion-controlled reaction.

Oxygen Kinetic Isotope Effects (^{18}*O KIEs*). ^{18}O KIEs were determined under competitive conditions using natural abundance O_2 as outlined in Materials and Methods. In all experiments, O_2 isolated subsequent to the enzymatic reaction was found to be enriched in ^{18}O. The reactions, therefore, are characterized by "normal" kinetic isotope effects where ^{16}O−^{16}O reacts faster than ^{18}O−^{16}O. The data are shown in Figure 9 where ^{18}O enrichment increases as an exponential function of the fractional conversion. This observation is consistent with eq 5 and the contribution of the isotopically sensitive step(s) to $k_{cat}/K_M(O_2)$ remaining unchanged as O_2 is consumed. Experiments with different preparations of enzyme and fatty acid substrate indicate $[k_{cat}/K_M(^{16}O-^{16}O)]/[k_{cat}/K_M(^{18}O-^{16}O)] = 1.0141 \pm 0.0011$ for AA and 1.0133 ± 0.0020 for LA. The small errors are typical for competitive isotope fractionation measurements.

The ^{18}O KIEs observed for AA and LA indicate that O_2 is reduced in or before the first irreversible step included within $k_{cat}/K_M(O_2)$. Equilibrium oxygen isotope effects (^{18}O EIEs) calculated from stretching frequencies are generally used to provide boundary conditions for interpreting the kinetic values (*54*). Relevant model reactions where O_2 is reduced to $HO_2^{\bullet}$, an allyl peroxyl radical, HO_2^-, and H_2O_2 are summarized in Table 2. The calculations indicate that the EIE should increase with the extent of O−O reduction and be attenuated by the formation of new bonds to oxygen concomitant with electron transfer.

The ^{18}O KIE $= 1.0133 \pm 0.0020$ observed for the LA is within error of the EIEs expected for formation of a peroxyl radical intermediate (1.010) and a hydroperoxide product (1.009). Significantly larger ^{18}O EIEs characterize the formation of $O_2^{\bullet-}$ (1.033) and HO_2^- (1.034). With respect

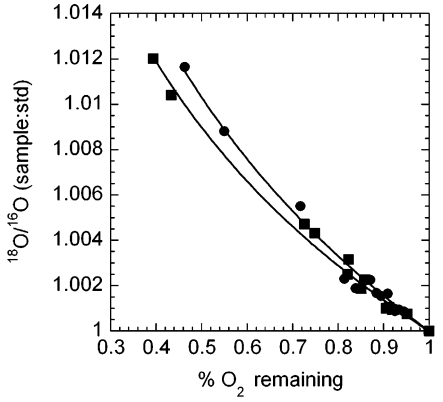

FIGURE 9: Isotope fractionation during the oxidation of AA (●) and LA (■) at pH 8 and 23 ± 2 °C. Data are fitted to the equation $(R_f/R_0) = (1 - f)^{exp}$, where exp = $1/^{18}$OKIE − 1.

Table 2: ^{18}O EIEs Calculated from Stretching Frequencies of the Reactant and Products (*54*, *69*)

Reaction	^{18}O EIE[a]
$O_2 + 1e^- \rightleftharpoons O_2^{\bullet -}$	1.033
$O_2 + H^\bullet \rightleftharpoons HO_2^\bullet$	1.010
O_2 + 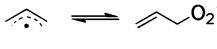	1.010
$O_2 + H^\bullet + e^- \rightleftharpoons HO_2^-$	1.034
$O_2 + 2H^\bullet \rightleftharpoons H_2O_2$	1.009

[a] Calculated for the $^{16}O-^{16}O$ and $^{18}O-^{16}O$ isotopologues.

to the ^{18}O KIE upon outer-sphere electron transfer to O_2, little deviation from the maximum EIE is expected (*70*).

It is not obvious why the ^{18}O KIE = 1.0141 ± 0.0011 for AA is similar to that observed for LA. In the case of AA, production of PGG_2 requires 2 equiv of O_2. As a result, the observed ^{18}O KIE reflects either one or two O_2-consuming steps. If O_2 were consumed before and after the first irreversible step within $k_{cat}/K_M(O_2)$, the observed ^{18}O KIE would be an average reflecting the two reactions; however, if the 2 equiv of O_2 were consumed in or before the first irreversible step, the observed ^{18}O KIE would be the product of an ^{18}O EIE and an ^{18}O KIE. The latter scenario would seem improbable since the O_2-consuming steps are most likely separated by an irreversible C−C bond-forming step, as discussed below.

Examination of $k_{cat}/K_M(O_2)$ as a Function of pH and pD. The dependence of $k_{cat}/K_M(O_2)$ upon lyonium ion concentration was examined at fatty acid concentrations >6 K_M (Figure 10). Above pH and pD 7, the rate profiles are flat, suggesting the absence of proton transfer. Kinetic solvent isotope effects are also undetectable in this region. Such isotope effects would be expected if either proton transfer or hydrogen atom transfer from a solvent-exchangeable site were to occur in a step which limits $k_{cat}/K_M(O_2)$. As the pL is decreased, however, a significant solvent isotope effect $^{H_2O}[k_{cat}/K_M(O_2)]/^{D_2O}[k_{cat}/K_M(O_2)] = 2.5 \pm 0.3$ is observed for LA. A smaller, perhaps insignificant, effect is observed for AA, $^{H_2O}[k_{cat}/K_M(O_2)]/^{D_2O}[k_{cat}/K_M(O_2)] = 1.4 \pm 0.2$. Studies at lower pH values are precluded by the poor solubility of the fatty acid.

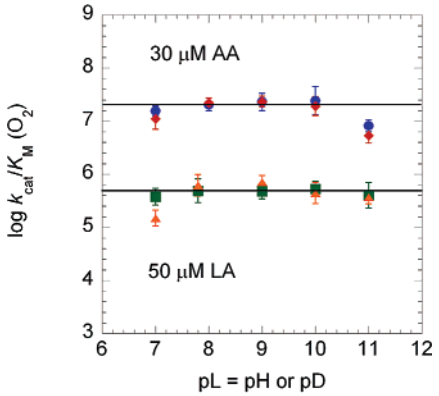

FIGURE 10: pL profiles of $k_{cat}/K_M(O_2)$ with AA in H_2O (●) or D_2O (◆) and LA in H_2O (■) or D_2O (▲). The horizontal lines represent the average $k_{cat}/K_M(O_2)$ between pH 8 and pH 10.

Deuterium Exchange Experiments. Experiments were undertaken to test the reversibility of initial H• abstraction from the fatty acid substrate. Specifically, it was of interest to determine whether deuterium from the D_2O solvent is incorporated into the substrate during the enzymatic reaction. Experiments under turnover conditions were performed using enzyme that had been dialyzed against ammonium acetate/D_2O buffer for 12 h at 4 °C. Reactions were allowed to proceed to 5−10% conversion before quenching and removal of the protein.

No evidence for exchange of deuterium from the solvent into the unreacted substrate is indicated by analysis of the fatty acids before and after the reaction with the enzyme. Each ESI mass spectrum is characterized by a major signal corresponding to the deprotonated fatty acid and accompanying signals at higher *m/z* due to the natural abundance levels of ^{13}C. The measured *m/z* ratios of 19.9 ± 0.6% (303/304) for AA and 15.8 ± 0.5% for LA (279/280) are somewhat lower than the theoretical ratios of 21.6% and 19.5% expected for the respective substrates. Analysis of the *m/z* ratios with fatty acid samples reisolated from reaction mixtures indicates values of 19.8 ± 1.1% for AA and 15.1 ± 0.8% for LA, which are not statistically different from those samples that had not been reacted with COX-1.

DISCUSSION

Amino acid residues in the active sites of dioxygenase enzymes are proposed to affect the positioning of substrates for initial activation as well as the selectivity of reactions involving O_2 (*71*−*75*). These features are illustrated by the ability of COX to convert a prochiral substrate (AA) into an oxidized and cyclized product with five chiral centers (PGG_2) (cf. eq 1). Elucidation of the kinetically reversible and irreversible steps is critical to understanding the cyclooxygenase mechanism which uniquely gives prostaglandin in preference to acyclic hydroperoxyeicosatetraenoic acids.

Proposals to explain the selective oxygenation reactions effected by COX-1 have been predicated on the idea that, subsequent to H• abstraction, O_2 reacts with the delocalized, substrate-derived radical in a highly regio- and stereospecific manner (*76*). The dominant site of attack is C-11 in AA and C-9 in LA at the face opposite from which the *pro-S* hydrogen is initially abstracted. O_2 trapping at C-15 in AA or C-13 in LA, at the same face of the delocalized radical, leads to hydroperoxide products having the *S* rather than *R*

stereochemistry (cf. eqs 1 and 2). Addition of O_2 to the carbon from which the H• is initially abstracted is also possible, but such products have not been observed.

Prostaglandin formation requires that cyclization of the 11*R*-peroxyl radical derived from AA outcompetes reduction to the 11-hydroperoxide. This 5-exo radical cyclization occurs by addition of the peroxyl oxygen to the C-9 double bond. Relative rates of cyclization to reduction can be estimated from the 95:5 ratio of PGG_2 to HpETE formed (*37*, *38*). The ratio of ~20 estimated from the products is comparable to the ratio of the $k_{cat}/K_M(O_2)$ values observed for AA and LA (cf. Table 1), consistent with divergent pathways subsequent to the formation of the 11 and the 9 or 13 peroxyl radicals.

Large-scale reorganization of the oxygenated intermediates must take place during AA oxidation. For instance, the first endoperoxide intermediate must rearrange to bring C-8 close enough to C-12 to form a new bond. This second cyclization is likely irreversible due to favorable thermodynamics associated with forming a C−C bond. In the third putative intermediate having the bicyclic endoperoxide structure, the radical equivalent has returned to its initial position at C-13. Addition of a second equivalent of O_2 to C-15 could then afford the 15-peroxyl radical which leads to the final product.

The regio- and stereospecific nature of the first O_2 addition step during AA oxygenation has been attributed to the following: (i) steric shielding of C-13 and C15, (ii) increased unpaired electron density at C-11, (iii) site-specific delivery of O_2 through channels within the protein, and (iv) reversible reaction of the substrate radical with O_2 and competitive kinetics downstream. Each of these possibilities has been evaluated using molecular dynamics simulations (*77*) with the finding that none of the first three proposals could independently account for the reaction selectivity. The mechanistic results presented in this work provide direct experimental support for proposal iv (*77*).

(I) Analysis of the Steady-State Kinetic Mechanism. The study of rate constants as a function of substrate concentration is frequently performed to illuminate enzyme kinetic mechanisms. To our knowledge, such systematic experiments had not been conducted with either form of COX. This work highlights the reproducible kinetic results which can be obtained using the slower substrate linoleic acid. Findings suggest that the dioxygenase reaction with this substrate is characterized by an apparent $k_{cat}/K_M(O_2)$ that depends upon the concentration of LA and an apparent $k_{cat}/K_M(LA)$ that depends upon the concentration of O_2. Further, experiments at different concentrations of phenol and hydroperoxide initiators provide no evidence for a decrease in the steady-state level of Tyr385• nor kinetic coupling of the dioxygenase and peroxidase reactions. Studies with the native substrate indicate that the apparent $k_{cat}/K_M(AA)$ depends upon the concentration of O_2 but that a change in the apparent $k_{cat}/K_M(O_2)$ is undetectable even at the lowest concentrations of AA examined. Together, the results appear to be most consistent with a sequential kinetic mechanism.

The steady-state kinetic results are inconsistent with a "ping-pong" mechanism in which the initial reaction of the fatty acid is kinetically uncoupled from the reaction with O_2; in this case, k_{cat}/K_M for each substrate should be insensitive to the concentration of the other. Such a mechanism would be expected if initial H• abstraction from the fatty acid were irreversible, as proposed for lipoxygenase enzymes which also catalyze the dioxygenation of LA (*78*, *79*). A sequential mechanism is, therefore, the preferred interpretation of the COX-1 kinetics, noting again the lack of experimental evidence for a pre-steady-state decline in the concentration of the Tyr385•.

The sequential mechanism in its most general form is defined according to the equation:

$$\frac{v}{[E]_T} = \frac{k_{cat}[A][B]}{K_{i,a}K_{M,B} + K_{M,B}[A] + K_{M,A}[B] + [A][B]} \quad (6)$$

which corresponds to a rapid equilibrium random mechanism; A and B are the substrates and $K_{i,a}$ is the inhibition constant for A (*80*). The expression predicts the hyperbolic behavior of the apparent second-order rate constants and can also account for the absence of a detectable decrease in $k_{cat}/K_M(O_2)$ upon decreasing the concentration of AA. In this case, tight binding of the native substrate such that $K_{i,a} \ll K_{M,A}$ is expected to make the first term in the denominator negligible, reducing the expression to one which resembles a ping-pong mechanism. Simplification of eq 6 also occurs when A binds rapidly with respect to B. In this case, $K_{M,A}$ approaches 0, and the system becomes ordered with the Michaelis constants approximating the substrate dissociation constants (*80*). The hallmark of such behavior is an insensitivity of k_{cat} to changes in the concentration of A, which is clearly not the case with COX-1.

The following discussion assumes the more general random substrate-binding mechanism, although the experimental results do not preclude a mechanism where binding of one substrate before the other is preferred (*80*). Regardless of the precise interpretation, the data obtained for COX-1 implicate a ternary complex of enzyme, fatty acid substrate, and O_2 as a kinetic intermediate prior to the first irreversible step (Scheme 2).

(II) Mechanism of Linoleic Acid Oxidation. The O_2-dependent steps after formation of the ternary complex were examined. The first step in k_p (referred to in Scheme 2) is assumed to be H• abstraction from the fatty acid. Direct insertion of O_2 into a C−H bond has a high kinetic barrier making activation of O_2 or the substrate required for oxygenation to proceed. In support of this assumption, EPR studies have demonstrated that Tyr385• reacts with stoichiometric AA to form an arachidonyl radical under anaerobic conditions (*81*, *82*), and studies with nitrone compounds have demonstrated trapping of the arachidonyl radical together with the inhibition of O_2 consumption (*83*). The oxidation of LA is the starting point for the following discussion as the reaction is simpler, involving only 1 equiv of O_2. A minimal chemical mechanism for this reaction is presented in Scheme 3.

(A) Evidence for Reversible H• Transfer. An important finding from this study concerns the reversibility of initial H• abstraction from the fatty acid (k_3 in Scheme 3). The sequential mechanism requires that O_2 and the fatty acid bind reversibly prior to the first kinetically irreversible step. Furthermore, the significant ^{18}O KIE (1.0133) observed for LA oxidation indicates a change in O−O bonding in or before this irreversible step. On these grounds, H• abstraction from LA by Tyr385• appears to be reversible. If the initial H• abstraction were irreversible, O_2 would be consumed in

Scheme 2: Random Sequential Mechanism for COX-1[a]

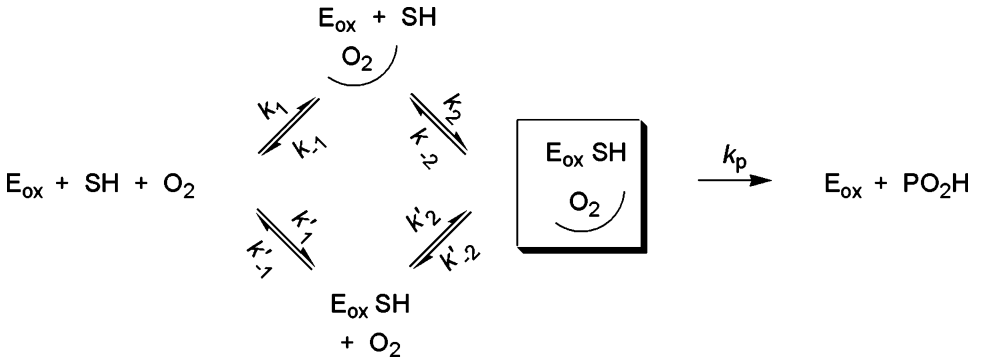

[a] E_{ox} = enzyme containing Tyr385•, SH = fatty acid, and PO_2H = hydroperoxide product.

Scheme 3: Microscopic Contributions to the O_2-Dependent Steps[a]

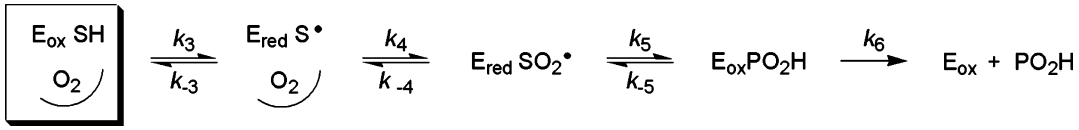

[a] k_p is defined in Scheme 2, E_{ox} = enzyme containing Tyr385•, SH = fatty acid, SO_2• = peroxyl radical intermediate, E_{red} = enzyme containing reduced Tyr385, and PO_2H = hydroperoxide product.

a reaction where no change in O−O bonding takes place and, thus, no ^{18}O KIE should be observed.

The reversibility of the initial H• transfer could, in principle, allow incorporation of deuterium from D_2O into the unreacted fatty acid substrate. Yet it has been difficult to obtain evidence for deuterium enrichment under turnover conditions. The negative result suggests that exchange between the catalytic Tyr385 and D_2O occurs on a longer time scale than enzyme turnover. Slow hydrogen exchange would not be surprising since Tyr385 resides in a hydrophobic pocket where it is hydrogen bonded to Tyr348 (*84*).

(B) Consideration of Substrate Binding and Product Release. Diffusion-controlled binding of the substrates and release of the hydroperoxide product are unlikely to contribute to the first kinetically irreversible step. The rates of these reactions would be expected to show a dependence upon solution viscosity, yet $k_{cat}/K_M(O_2)$ and k_{cat}/K_M(LA) are unchanged when the relative viscosity is increased 4-fold. That product release is not the first kinetically irreversible step is further supported by the absence of an effect upon $k_{cat}/K_M(O_2)$ when hydroperoxide initiators, present initially in the fatty acid substrates, are added in excess to the assay solutions.

(C) Formation of the Peroxyl Radical Intermediate. Another possibility for the first kinetically irreversible step is formation of the peroxyl radical upon trapping of the delocalized substrate-derived radical by O_2 (k_4 in Scheme 3). Although this result seems at odds with the viscosity studies, it has been suggested that prebinding of O_2 in a cavity near the active site followed by its migration to the substrate-derived radical would not show the dependence upon added solvent viscosogen anticipated for a bimolecular, diffusion-controlled reaction (*79*).

The related solution-phase reaction of O_2 and the linoleyl radical is reversible according to studies by Porter and coworkers (*85*, *86*). In this reaction, oxygenation of C-9, C-11, and C-13 occurs with rate constants that approach the diffusion limit. The reverse (β-scission) reaction occurs with rate constants ranging from 10^2 to 10^7 s^{-1} depending on the stability of the peroxyl radical. In light of the comparison to the solution-phase reaction, it is difficult to attribute $k_{cat}/K_M(O_2) = 5.6 \times 10^5$ M^{-1} s^{-1} determined for the COX-1 reaction with LA to O_2 trapping. Unfavorable preequilibria associated with forming the enzyme-bound substrate radical complex could, however, dramatically reduce the rate constant from that expected for a diffusion-controlled reaction. Such behavior cannot be strictly ruled out within the context of the sequential kinetic mechanism, yet seems unlikely in view of the thermodynamics associated with H• transfer from the fatty acid to Tyr385• (see below).

A final observation related to O_2 trapping concerns the closeness of the observed ^{18}O KIE (1.0133) to the upper limit EIEs calculated (~1.01) for forming a peroxyl radical or a hydroperoxide product. Given the barrier-less nature of the solution reaction between the linoleyl radical and O_2, the closeness of the KIE to the EIE is difficult to attribute to a product-like transition state in the enzymatic reaction. Rather, the favored explanation involves reversible trapping of the substrate radical by O_2 prior to an irreversible step characterized by a small ^{18}O KIE.

(D) Reduction of the Peroxyl Radical Intermediate. The pH and pD profiles of $k_{cat}/K_M(O_2)$ address the involvement of peroxyl radical reduction in the first kinetically irreversible step in the mechanism of Scheme 3. This reoxidation step requires either outer-sphere electron transfer or H• transfer from the Tyr385 to the peroxyl radical.

If reduction of the fatty acid peroxyl radical were to occur by electron transfer, a significant change in $k_{cat}/K_M(O_2)$ might be observed as the pH is raised in the region of the tyrosine pK_a (*87*). The tyrosinate is expected to react by electron transfer faster than the neutral residue due to its lower one-electron redox potential (*88*). Yet, if electron transfer were to occur at a rate similar to hydrogen atom transfer from the reduced neutral tyrosine (see below), $k_{cat}/K_M(O_2)$ might appear to be independent of pH. A further uncertainty concerns how the magnitude of the ^{18}O KIE would be affected by rapid outer-sphere electron transfer subsequent to reversible formation of the peroxyl radical. Thus, we leave

open the possibility that the first irreversible step involves electron transfer from Tyr385.

Reduction of the fatty acid peroxyl radical by H• transfer is consistent with the size of the ^{18}O KIE and the limit set by the ^{18}O EIE for forming a hydroperoxide product. This reaction might not be characterized by a pH dependence although kinetic solvent isotope effects upon $k_{cat}/K_M(O_2)$ would be expected. Such an effect is observed upon $k_{cat}/K_M(O_2)$ at pL 7 with LA but not with AA. The result cannot be unambiguously assigned to a kinetic solvent isotope effect since perturbing the interaction between the fatty acid carboxylate ($pK_a \sim 7$) (*89*) and the catalytically important arginine (Arg120) (*90*) could cause the same behavior. The observation that solvent isotope effects are absent at the higher pH values is more difficult to explain but could reflect an increased contribution due to the electron transfer mechanism described above.

Finally, an irreversible conformational change in the first kinetically irreversible step of LA oxidation is difficult to rule out. Large-scale rearrangement is necessary to facilitate H• transfer from Tyr385 to the 9- and 13-peroxyl radicals derived from LA. This possibility has previously been discussed for a lipoxygenase enzyme which shows many similar features to COX-1 as described below (*79*). Conformational gating might allow the peroxyl radical to selectively abstract an H• from Tyr385 rather than other oxidizable amino acid residues in close proximity (e.g., Trp387 or Tyr348).

(III) Arachidonic Acid Oxidation. The formation of the bicyclic endoperoxide structure with new C−O and C−C bonds differentiates AA oxidation from LA oxidation. The cyclization steps require significant reorganization of the oxygenated intermediates in the enzyme active site (*91*). The small viscosity effects upon $k_{cat}/K_M(O_2)$ and $k_{cat}/K_M(AA)$ may reflect a substrate-based conformational change, i.e., 5-exo radical cyclization, as the first kinetically irreversible step. This step precedes reduction of the terminal peroxyl radical, and therefore, no pH dependence or solvent kinetic isotope effect would be expected.

The sequential steady-state kinetic mechanism is consistent with common steps leading up to the formation of the first peroxyl radical intermediate during the oxidation of AA and LA. In both cases, H• transfer is proposed to occur reversibly before O_2 enters the catalytic cycle. This proposal explains the magnitudes of the ^{18}O KIEs of 1.0141 (AA) and 1.0133 (LA), both of which are consistent with a reversible reaction of the substrate radical and O_2 prior to an irreversible step exhibiting a small KIE.

The results point toward cyclization to form either the five-membered endoperoxide ring or the bicyclic endoperoxide structure as the first irreversible step in AA oxygenation whereas this step may involve peroxyl radical reduction in the case of LA. The origin of specificity in the AA reaction is, therefore, visualized in terms of O_2 trapping in competition with reversible H• transfer. In contrast, if initial C−H activation were kinetically irreversible under the conditions examined, the delocalized arachidonyl radical that accumulated during enzyme turnover would be susceptible to competing reaction pathways leading to HpETE products rather than PGG_2.

(A) Thermodynamic Considerations. The thermodynamics of the initial H• abstraction is expected to be similar for AA and LA based on the bisallylic homolytic C−H bond strengths (ca. 80 kcal mol^{-1}) of 1,4-pentadiene in solution (*92*) as well as the similar rate constants observed for these substrates in other enzyme reactions (*93*). The H• affinity of the tyrosyl radical or inverse of the tyrosine O−H bond strength is generally viewed as somewhat higher (82 to ∼88 kcal mol^{-1}) (*24*, *94*, *95*) than that of the bisallylic C−H. The thermodynamics of H• transfer could, however, be altered within the enzyme active site due to interactions which stabilize the tyrosyl radical. Recent high-field EPR and ENDOR studies have provided evidence that hydrogen bonding occurs between the −OH of Tyr348 and Tyr385• (*96*). Such stabilization would make Tyr385• a poorer oxidant but favor its selective oxidation by $Fe^{IV}(O)Por^{•+}$ in the presence of other residues capable of losing an electron as well as a proton.

(B) Deuterium Kinetic Isotope Effect Studies. In the literature, C−H oxidation has been considered an initial and "rate-limiting" step in cyclooxygenase catalysis. This idea has been based on a competitive tritium isotope effect of $^{H}[k_{cat}/K_M]/^{T}[k_{cat}/K_M] \sim 4$ estimated from the early work of Hamberg and Samuelsson (*35*), who measured isotope fractionation of starting material in the reaction of microsomal COX-1 with specifically labeled 8,11,14-eicosatrienoic acids. Yet at this time the experiments required to interpret competitive KIEs in terms of steady-state microscopic rate constants had not been clarified (*97*). Of particular significance is the frequently obscured relationship between the observed KIE and the intrinsic KIE on the chemical step. This parameter cannot simply be extracted from the competitive KIE without knowledge of the forward and reverse commitments to catalysis, both of which can suppress the intrinsic KIE.

The competitive tritium isotope effect on the COX reaction is much smaller than the intrinsic H/T KIE of ca. 15 expected for C−H cleavage as well as the very large intrinsic H/D KIEs of ∼80 reported for related reactions of lipoxygenase enzymes (*98*, *99*). One possible explanation is that the small KIE on the COX-1 reaction arises from a large forward commitment to catalysis, in other words, slow release of the substrate from the enzyme relative to the product-forming step. Another possibility is that the isotope effect is influenced by the reverse commitment factor with the chemical step approaching equilibrium. A rapid equilibrium C−H−O hydrogen atom transfer prior to the first kinetically irreversible step would be expected to exhibit an equilibrium isotope effect <2 (*100*), though significant deviations have been observed in cases where a proton donor interacts strongly with an acceptor through what appears to be a low-barrier hydrogen bond (*101*). Examining the relationship of the KIEs upon k_{cat} and k_{cat}/K_M to the intrinsic KIE on C−H oxidation of LA should further illuminate the proposed mechanism.

(IV) Comparisons to Lipoxygenase. Cyclooxygenase and lipoxygenase enzymes are found colocalized within the nucleus of the cell where they compete for O_2 as well as AA (*102*). The enzymes are ancestrally unrelated and exhibit no structural homology (*103*), yet appear to react by similar mechanisms. Extensive studies with soybean lipoxygenase (LOX-1) and its native substrate LA have revealed $k_{cat} = 230 \pm 15\ s^{-1}$, $k_{cat}/K_M(LA) = (13 \pm 2) \times 10^6\ M^{-1}\ s^{-1}$, and $k_{cat}/K_M(O_2) = (21 \pm 1) \times 10^6\ M^{-1}\ s^{-1}$ at 20 °C (*78*, *79*). In addition, $k_{cat}/K_M(O_2)$ is unaffected by changes in solvent pH,

pD, and viscosity. An ^{18}O KIE of 1.0115 ± 0.0013 has been reported and suggested to arise from either kinetically irreversible trapping of the delocalized substrate radical by O_2 or a downstream conformational change. The kinetics of AA oxidation by human lipoxygenases appears to be similar (*104*) although studies of the oxygenation mechanism have not been reported.

The kinetic parameters for lipoxygenase bear a resemblance to those observed for COX-1 reacting with its native substrate AA (cf. Table 1). Yet, in contrast, LOX is believed to react by a ping-pong kinetic mechanism with irreversible H• abstraction preceding O_2 trapping of the delocalized linoleyl radical intermediate (*79*). Arguments against the sequential kinetic mechanism have been based on the observations of large primary deuterium KIEs on k_{cat}/K_M(LA) and k_{cat} but not $k_{cat}/K_M(O_2)$. In spite of the difference in the kinetic mechanism, COX and LOX seem to mediate substrate oxidation in similar ways. In LOX, a high-potential non-heme iron hydroxide cofactor (*105*) appears to initiate fatty acid oxygenation by H• abstraction. In COX, the H• abstractor appears to be a tyrosyl radical. Neither of the cofactors reacts directly with O_2 during catalysis, and both undergo activation through reactions involving hydroperoxide compounds.

The oxidants in COX and LOX effect the removal of an H• from the bisallyic position of the fatty acid by accepting a proton and an electron ($H^\bullet \equiv H^+ + e^-$). The thermodynamic H• affinity of the $Fe^{III}OH$ in LOX-1 has been estimated to be 85 kcal mol^{-1} (*106*), which is within the range expected for a tyrosyl radical (*24*). The intrinsic barriers also appear to be similar for converting $Fe^{III}(L)$ to $Fe^{II}(LH)$ and phenoxyl radicals to phenols (*107*). Computational studies have confirmed these results and suggested reorganization energies for coupled electron/proton transfer of 20−30 kcal mol^{-1} (*108*, *109*). In the absence of large differences in the hydrogen tunneling probabilities, similar H• abstraction rate constants ($k_{H^\bullet}$) are anticipated for fatty acid oxidation by the two enzymes. The $k_{H^\bullet} = 230\ s^{-1}$ reported for LOX-1 (*105*) and the lower limit of $k_3 > 73.5\ s^{-1}$ estimated on the basis of k_{cat} for COX-1 are consistent with this expectation.

To account for the reversibility of H• transfer in COX-1 within the context of Scheme 3, the reverse H• transfer (k_{-3}) must compete with O_2 trapping of the substrate radical (k_4). This situation would obtain if the effective concentration of O_2 able to reach C-11 were very low or if the reverse H• abstraction from Tyr385 were very fast. As discussed above, the mechanistic results are consistent with the latter, suggesting that the thermodynamics of the C−H oxidation in COX-1 might be less favorable than in LOX-1 by a few kilocalories per mole. A reduced H• affinity relative to the iron cofactor most likely relates to the requirement that the tyrosyl radical be selectively generated by long-range electron transfer to $Fe^{IV}(O)Por^{\bullet+}$ whereas LOX is activated through a direct reaction of the hydroperoxide product with the ferrous cofactor. Furthermore, the oxidizing ability of the Tyr385• in COX is likely tuned to accommodate its persistence and kinetic competence to effect C−H homolysis in the presence of other oxidizable amino acid residues.

CONCLUSIONS

Molecular oxygen-dependent steps during COX-1 catalysis have been examined with arachidonic acid and linoleic acid as substrates. Under the experimental conditions, the dioxygenase and peroxidase reactions occur independently, and there is no evidence for a decline in the steady-state concentration of the active enzyme. Mechanistic probes, including studies of the enzyme kinetics at varying substrate concentrations and competitive oxygen kinetic isotope effects, were employed in this work.

The results are consistent with a sequential kinetic mechanism involving formation of a ternary complex of enzyme, fatty acid substrate, and O_2. The observed competitive oxygen kinetic isotope effect imposes the additional constraint that a change in O−O bonding occurs in or before the first kinetically irreversible step. It follows from these observations that initial H• abstraction from the fatty acid by the tyrosyl radical occurs reversibly prior to the reaction of O_2. Furthermore, the magnitudes of competitive oxygen kinetic isotope effects observed with two fatty acid substrates suggest that O_2 reacts reversibly and that a downstream step determines the identities of the products formed.

An implication from these studies is that the specificity of fatty acid oxygenation does not require irreversible trapping of the substrate-derived radical by O_2. In the case of arachidonic acid, the first kinetically irreversible step, proposed to facilitate formation of prostaglandin G_2 rather than hydroperoxyeicosatetraenoic acids, is either the first cyclization leading to the five-membered endoperoxide ring or the second cyclization leading to the bicyclic endoperoxide intermediate. For linoleic acid, the first irreversible step is proposed to be reduction of the peroxyl radical or a prior conformational change involving this species. In summary, the results highlight the importance of kinetic factors in determining the regio- and stereospecific nature of O_2 reactions in cyclooxygenase enzymes.

SUPPORTING INFORMATION AVAILABLE

Eleven figures providing additional kinetic plots. This material is available free of charge via the Internet at http://pubs.acs.org.

REFERENCES

1. Rouzer, C. A., and Marnett, L. J. (2003) Mechanism of free radical oxygenation of polyunsaturated fatty acids by cyclooxygenases, *Chem. Rev. 103*, 2239−2304.
2. Funk, C. D. (2001) Prostaglandins and leukotrienes: advances in eicosanoid biology, *Science 294*, 1871−1875.
3. Lambeir, A. M., Markey, C. M., Dunford, H. B., and Marnett, L. J. (1985) Spectral properties of the higher oxidation states of prostaglandin H-synthase, *J. Biol. Chem. 260*, 14894−14896.
4. Gao, L., Zackert, W. E., Hasford, J. J., Danekis, M. E., Milne, G. L., Remmert, C., Reese, J., Yin, H., Tai, H.-H., Dey, S. K., Porter, N. A., and Morrow, J. D. (2003) Formation of prostaglandins E2 and D2 via the isoprostane pathway: A mechanism for generation of bioactive prostaglandins independent of cyclooxygenase, *J. Biol. Chem. 278*, 28479−28489.
5. Smith, W. L., Dewitt, D. L., and Garvito, R. M. (2000) Cyclooxygenases: structural, cellular, and molecular biology, *Annu. Rev. Biochem. 69*, 145−182.
6. Vane, J. R., Bakhle, Y. S., and Botting, R. M. (1998) Cyclooxygenases 1 and 2, *Annu. Rev. Pharmacol. Toxicol. 38*, 97−120.
7. Rouzer, C. A., and Marnett, L. J. (2005) Structural and functional differences between cyclooxygenases: Fatty acid oxygenases with a critical role in cell signaling, *Biochem. Biophys. Res. Commun. 338*, 34−44.
8. Simmons, D. L., Botting, R. M., and Hla, T. (2004) Cyclooxygenase isozymes: the biology of prostaglandin synthesis and inhibition, *Pharmacol. Rev. 56*, 387−438.

9. Nagano, S., Huang, X., Moir, R. D., Payton, S. M., Tanzi, R. E., and Bush, A. I. (2004) Peroxidase activity of cyclooxygenase-2 (COX-2) cross-links β-amyloid (Aβ) and generates Aβ-COX-2 hetero-oligomers that are increased in Alzheimer's disease, *J. Biol. Chem. 279*, 14673−14678.
10. Prescott, S. M., and Fitzpatrick, F. A. (2000) Cyclooxygenase-2 and carcinogenesis, *Biochim. Biophys. Acta 1470*, M69−M78.
11. Karthein, R., Dietz, R., Nastainczyk, W., and Ruf, H. H. (1988) Higher oxidation states of prostaglandin H synthase. EPR study of a transient tyrosyl radical in the enzyme during the peroxidase reaction, *Eur. J. Biochem. 171*, 313−320.
12. Dietz, R., Nastainczyk, W., and Ruf, H. H. (1988) Higher oxidation states of prostaglandin H synthase. Rapid electronic spectroscopy detected two spectral intermediates during the peroxidase reaction with prostaglandin G2, *Eur. J. Biochem. 171*, 321−328.
13. Shimokawa, T., Kulmacz, R. J., DeWitt, D. L., and Smith, W. L. (1990) Tyrosine 385 of prostaglandin endoperoxide synthase is required for cyclooxygenase catalysis, *J. Biol. Chem. 265*, 20073−20076.
14. Tsai, A.-L., and Kulmacz, R. J. (2000) Tyrosyl radicals in prostaglandin H synthase-1 and -2, *Prostaglandins Other Lipid Mediators 62*, 231−254.
15. Tsai, A.-L., His, L. C., Kulmacz, R. J., Palmer, G., and Smith, W. L. (1994) Characterization of the tyrosyl radicals in ovine prostaglandin H synthase-1 by isotope replacement and site-directed mutagenesis, *J. Biol. Chem. 269*, 5085−5091.
16. Hsi, L. C., Hoganson, C. W., Babcock, G. T., Garavito, R. M., and Smith, W. L. (1995) An examination of the source of the tyrosyl radical in ovine prostaglandin endoperoxide synthase-1, *Biochem. Biophys. Res. Commun. 207*, 652−660.
17. Shi, W., Hoganson, C. W., Espe, M., Bender, C. J., Babcock, G. T., Palmer, G., Kulmacz, R. J., and Tsai, A.-L. (2000) Electron paramagnetic resonance and electron nuclear double resonance spectroscopic identification and characterization of the tyrosyl radicals in prostaglandin H synthase 1, *Biochemistry 39*, 4112−4121.
18. Lassmann, G., Odenwaller, R., Curtis, J. F., DeGray, J. A., Mason, R. P., Marnett, L. J., and Eling, T. E. (1991) Electron spin resonance investigation of tyrosyl radicals of prostaglandin H synthase: Relation to enzyme catalysis, *J. Biol. Chem. 266*, 20045−20055.
19. DeGray, J. A., Lassmann, G., Curtis, J. F., Kennedy, T. A., Marnett, L. J., Eling, T. E., and Mason, R. P. (1992) Spectral analysis of the protein-derived tyrosyl radicals from prostaglandin H synthase, *J. Biol. Chem. 267*, 23583−23588.
20. Tsai, A.-L., Wu, G., Palmer, G., Bambai, B., Koehn, J. A., Marshall, P. J., and Kulmacz, R. J. (1999) Rapid kinetics of tyrosyl radical formation and heme redox state changes in prostaglandin H synthase-1 and -2, *J. Biol. Chem. 274*, 21695−21700.
21. Malkowski, M. G., Ginell, S. L., Smith, W. L., and Garavito, R. M. (2000) The productive conformation of arachidonic acid bound to prostaglandin synthase, *Science 289*, 1933−1937.
22. Rogge, C. E., Liu, W., Wu, G., Wang, L.-H., Kulmacz, R. J., and Tsai, A.-L. (2004) Identification of Tyr504 as an alternative tyrosyl radical site in human prostaglandin H synthase-2, *Biochemistry 43*, 1560−1568.
23. Rogge, C. E., Ho, B., Liu, W., Kulmacz, R. J., and Tsai, A.-L. (2006) Role of Tyr348 in Tyr385 radical dynamics and cyclooxygenase inhibitor interactions in prostaglandin H synthase-2, *Biochemistry 45*, 523−532.
24. Stubbe, J., and van der Donk, W. A. (1998) Protein radicals in enzyme catalysis, *Chem. Rev. 98*, 705−762.
25. Svistunenko, D. A. (2005) Reaction of heme containing proteins and enzymes with hydroperoxides: The radical view, *Biochim. Biophys. Acta 1707*, 127−155.
26. Schuenemann, V., Lendzian, F., Jung, C., Contzen, J., Barra, A.-L., Sligar, S. G., and Trautwein, A. X. (2004) Tyrosine radical formation in the reaction of wild type and mutant cytochrome P450cam with peroxy acids: A multifrequency EPR study of intermediates on the millisecond time scale, *J. Biol. Chem. 279*, 10919−10930.
27. Yu, S., Girotto, S., Zhao, X., and Magliozzo, R. S. (2003) Rapid formation of compound II and a tyrosyl radical in the Y229F mutant of *Mycobacterium tuberculosis* catalase-peroxidase disrupts catalase but not peroxidase function, *J. Biol. Chem. 278*, 44121−44127.
28. Jakopitsch, C., Ivancich, A., Schmuckenschlager, F., Wanasinghe, A., Pöltl, G., Furtmüller, P. G., Rüker, F., and Obinger, C. (2004) Influence of the unusual covalent adduct on the kinetics and formation of radical intermediates in *Synechocystis* catalase peroxidase. A stopped-flow and EPR characterization of the Met275, Tyr249, and Arg439 variants, *J. Biol. Chem. 279*, 46082−46095.
29. Ehrenshaft, M., and Mason, R. P. (2006) Protein radical formation on thyroid peroxidase during turnover as detected by immuno-spin trapping, *Free Radical Biol. Med. 41*, 422−430.
30. Su, C., Sahlin, M., and Oliw, E. H. (1998) A protein radical and ferryl intermediates are generated by linoleate diol synthase, a ferric hemeprotein with dioxygenase and hydroperoxide isomerase activities, *J. Biol. Chem. 273*, 20744−20751.
31. Hamberg, M., Sanz, A., and Castresana, C. (2002) α-Dioxygenase, a new enzyme in fatty acid metabolism, *Int. Cong. Ser. 1233*, 307−317.
32. Koeduka, T., Matsui, K., Akakabe, Y., and Kajiwara, T. (2002) Catalytic properties of rice α-oxygenase: a comparison with mammalian prostaglandin H synthases, *J. Biol. Chem. 277*, 22648−22655.
33. Liu, W., Rogge, C. E., Bambai, B., Palmer, G., Tsai, A.-L., and Kulmacz, R. J. (2004) Characterization of the heme environment in *Arabidopsis thaliana* fatty acid α-dioxygenase-1, *J. Biol. Chem. 279*, 29805−29815.
34. Malkowski, M. G., Thuresson, E. D., Lakkides, K. M., Rieke, C. J., Micielli, R., Smith, W. L., and Garavito, R. M. (2001) Structure of eicosapentaenoic and linoleic acids in the cyclooxygenase site of prostaglandin endoperoxide H synthase-1, *J. Biol. Chem. 276*, 37547−37555.
35. Hamberg, M., and Samuelsson, B. (1967) On the mechanism of the biosynthesis of prostaglandins E-1 and F-1-alpha, *J. Biol. Chem. 242*, 5336−5343.
36. Hamberg, M., and Samuelsson, B. (1980) Stereochemistry in the formation of 9-hydroxy-10,12-octadecadienoic acid and 13-hydroxy-9,11-octadecadienoic acid from linoleic acid by fatty acid cyclooxygenase, *Biochim. Biophys. Acta 617*, 545−547.
37. Thuresson, E. D., Lakkides, K. M., and Smith, W. L. (2000) Different catalytically competent arrangements of arachidonic acid within the cyclooxygenase active site of prostaglandin endoperoxide H synthase-1 lead to the formation of different oxygenated products, *J. Biol. Chem. 275*, 8501−8507.
38. Smith, W. L., and Song, I. (2002) The enzymology of prostaglandin endoperoxide H synthases-1 and -2, *Prostaglandins Other Lipid Mediators 68*, 115−128.
39. Hamberg, M. (1998) Stereochemistry of oxygenation of linoleic acid catalyzed by prostaglandin−endoperoxide H synthase-2, *Arch. Biochem. Biophys. 349*, 376−380.
40. Marnett, L. J., Siedlik, P. H., Ochs, R. C., Pagels, W. R., Das, M., Honn, K. V., Warnock, R. H., Tainer, B. E., and Eling, T. E. (1984) Mechanism of the stimulation of prostaglandin H synthase and prostacyclin synthase by the antithrombotic and antimetastatic agent, nafazatrom, *Mol. Pharmacol. 26*, 328−335.
41. Kulmacz, R. J., and Lands, W. E. M. (1984) Prostaglandin H synthase. Stoichiometry of heme cofactor, *J. Biol. Chem. 259*, 6358−6363.
42. Xiao G. S., Chen W., and Kulmacz R. J. (1998) Comparison of structural stabilities of prostaglandin H synthase-1 and -2, *J. Biol. Chem. 273*, 6801−6811.
43. Rome, L. H., and Lands, W. E. M. (1975) Structural requirements for time-dependent inhibition of prostaglandin biosynthesis by anti-inflammatory drugs, *Proc. Natl. Acad. Sci. U.S.A. 72*, 4863−4865.
44. Kulmacz, R. J., and Lands, W. E. M. (1985) Stoichiometry and kinetics of the interaction of prostaglandin H synthase with anti-inflammatory agents, *J. Biol. Chem. 260*, 12572−12578.
45. Hsuanyu, Y., and Dunford, B. H. (1992) Prostaglandin H synthase kinetics. The effect of substituted phenols on cyclooxygenase activity and the substituent effect on phenolic peroxidatic activity, *J. Biol. Chem. 267*, 17649−17657.
46. Kulmacz, R. J., Pendleton, R. B., and Lands, W. E. M. (1994) Interaction between peroxidase and cyclooxygenase activities in prostaglandin−endoperoxide synthase. Interpretation of reaction kinetics, *J. Biol. Chem. 269*, 5527−5536.
47. Bakovic, M., and Dunford, B. H. (1996) Effect of Trolox C on the oxygenation reaction of prostaglandin endoperoxide synthase with *cis,cis*-eicosa-11,14-dienoic acid, *Prostaglandins, Leukotrienes Essent. Fatty Acids 54*, 341−349.
48. Kulmacz, R. J., van der Donk, W. A., and Tsai, A.-L. (2003) Comparison of the properties of prostaglandin H synthase-1 and -2, *Prog. Lipid Res. 42*, 377−404.

49. Wei, C., Kulmacz, R. J., and Tsai, A.-L. (1995) Comparison of branched-chain and tightly coupled reaction mechanisms for prostaglandin H synthase, *Biochemistry 34*, 8499−8512.
50. Bambai, B., and Kulmacz, R. J. (2000) Prostaglandin H synthase. Effects of peroxidase cosubstrates on cyclooxygenase velocity, *J. Biol. Chem. 275*, 27608−27614.
51. Brouwer, A. C., and Kirsch, J. F. (1982) Investigation of diffusion-limited rates of chymotrypsin reactions by viscosity variation, *Biochemistry 21*, 1302−1307.
52. Hasinoff, B. B., and Chishti, S. B. (1982) Viscosity dependence of the kinetics of the diffusion-controlled reaction of carbon monoxide and myoglobin, *Biochemistry 21*, 4275−4278.
53. Dunford, H. B., and Hasinoff, B. B. (1986) On the rates of enzymatic, protein and model compound reactions: the importance of diffusion control, *J. Inorg. Biochem. 28*, 263−269.
54. Roth, J. P., and Klinman, J. P. (2006) Oxygen kinetic isotope effects as probes of enzymatic activation of molecular oxygen, in *Isotope Effects in Chemistry and Biology* (Kohen, A., and Limbach, H.-H. Eds.) pp 645−669, CRC Press, Boca Raton, FL.
55. Goodwin, D. C., Rowlinson, S. W., and Marnett, L. J. (2000) Substitution of tyrosine for the proximal histidine ligand to the heme of prostaglandin endoperoxide synthase 2: Implications for the mechanism of cyclooxygenase activation and catalysis, *Biochemistry 39*, 5422−5432.
56. Koshkin, V., and Dunford, H. B. (1999) Coupling of the peroxidase and cyclooxygenase reactions of prostaglandin H synthase, *Biochim. Biophys. Acta 1430*, 341−348.
57. Kulmacz, R. J. (2005) Regulation of cyclooxygenase catalysis by hydroperoxides, *Biochem. Biophys. Res. Commun. 338*, 25−33.
58. Kulmacz, R. J., Pendleton, R. B., and Lands, W. E. M. (1994) Interaction between peroxidase and cyclooxygenase activities in prostaglandin−endoperoxide synthase. Interpretation of reaction kinetics, *J. Biol. Chem. 269*, 5527−5536.
59. Lu, G., Tsai, A.-L., Van Wart, H. E., and Kulmacz, R. J. (1999) Comparison of the peroxidase reaction kinetics of prostaglandin H synthase-1 and -2, *J. Biol. Chem. 274*, 16162−16167.
60. Kulmacz, R. J., Palmer, G., and Tsai, A.-L. (1991) Prostaglandin H synthase: perturbation of the tyrosyl radical as a probe of anticyclooxygenase agents, *Mol. Pharmacol. 40*, 833−837.
61. Laneuville, O., Breuer, D. K., Xu, N., Hunag, Z. H., Gage, D. A., Watson, J. T., Lagarde, M., DeWitt, D. L., and Smith, W. L. (1995) Fatty acid substrate specificities of human prostaglandin-endoperoxide H synthase-1 and -2, *J. Biol. Chem. 270*, 19330−19336.
62. Koshkin, V., and Dunford, B. H. (1998) Reaction of prostaglandin endoperoxide synthase with *cis*,*cis*-eicosa-11,14-dienoic acid, *J. Biol. Chem. 273*, 6046−6049.
63. Hemler, M. E., Crawford, C. G., and Lands, W. E. M. (1978) Lipoxygenation activity of purified prostaglandin-forming cyclooxygenase, *Biochemistry 17*, 1772−1779.
64. Smith, W. L., and Lands, W. E. M. (1972) Oxygenation of polyunsaturated fatty acids during prostaglandin biosynthesis by sheep vesicular glands, *Biochemistry 11*, 3276−3285.
65. Juránek, I., Suzuki, H., and Yamamoto, S. (1999) Affinities of various mammalian arachidonate lipoxygenases and cyclooxygenases for molecular oxygen as substrate, *Biochim. Biophys. Acta 1436*, 509−518.
66. Song, I., Ball, T. M., and Smith, W. L. (2001) Different suicide inactivation processes for the peroxidase and cyclooxygenase activities of prostaglandin endoperoxide H synthase-1, *Biochem. Biophys. Res. Commun. 289*, 869−875.
67. Swinney, D. C., Mak, A., Barnett, J., and Ramesha, C. S. (1997) Differential allosteric regulation of prostaglandin H synthase 1 and 2 by arachidonic acid, *J. Biol. Chem. 272*, 12393−12398.
68. Chen, W., Pawelek, T. R., and Kulmacz, R. J. (1999) Hydroperoxide dependence and cooperative cyclooxygenase kinetics in prostaglandin H synthase-1 and -2, *J. Biol. Chem. 274*, 20301−20306.
69. Baskir, E. G., and Nefedov, O. M. (1996) IR spectroscopic study of allylperoxy radical and products of its phototransformations in the Ar matrix, *Russ. Chem. Bull. 45*, 99−107.
70. Roth, J. P. (2007) Advances in studying bioinorganic reaction mechanisms: Isotopic probes of activated oxygen intermediates in metalloenzymes, *Curr. Opin. Chem. Biol.* (in press).
71. Thuresson, E. D., Lakkides, K. M., Rieke, C. J., Sun, Y., Wingerd, B. A., Micielli, R., Mulichak, A. M., Malkowski, M. G., Garavito, R. M., and Smith, W. L. (2001) Prostaglandin endoperoxide H synthase-1. The functions of cyclooxygenase active site residues in the binding, positioning and oxygenation of arachidonic acid, *J. Biol. Chem. 276*, 10347−10359.
72. Schneider, C., and Brash, A. R. (2000) Stereospecificity of hydrogen abstraction in the conversion of arachidonic acid to 15R-HETE by Aspirin-treated cyclooxygenase-2. Implications for the alignment of substrate in the active site, *J. Biol. Chem. 275*, 4743−4746.
73. Knapp, M. J., Seebeck, F. P., and Klinman, J. P. (2001) Temperature-dependent isotope effects in soybean lipoxygenase-1: Correlating hydrogen tunneling with protein dynamics, *J. Am. Chem. Soc. 123*, 2931−2932.
74. Coffa, G., Imber, A. N., Maguire, B. C., Laxmikanthan, G., Schneider, C., Gaffney, B. J., and Brash, A. R. (2005) On the relationships of substrate orientation, hydrogen abstraction, and product stereochemistry in single and double dioxygenations by soybean lipoxygenase-1 and its Ala542Gly mutant, *J. Biol. Chem. 280*, 38756−38766.
75. Coffa, G., Schneider, C., and Brash, A. R. (2005) A comprehensive model of positional and stereo control in lipoxygenases, *Biochem. Biophys. Res. Commun. 338*, 87−92.
76. Kiefer, J. R., Pawlitz, J. L., Moreland, K. T., Stegeman, R. A., Hood, W. F., Gierse, J. K., Stevens, A. M., Goodwin, D. C., Rowlinson, S. W., Marnett, L. J., Stallings, W. C., and Kurumbail, R. G. (2000) Structural insights into the stereochemistry of the cyclooxygenase reaction, *Nature 405*, 97−101.
77. Furse, K. E., Pratt, D. A., Schneider, C., Brash, A. R., Porter, N. A., and Lybrand, T. P. (2006) Molecular dynamics simulations of arachidonic acid-derived pentadienyl radical intermediate complexes with COX-1 and COX-2: Insights into oxygenation regio- and stereoselectivity, *Biochemistry 45*, 3206−3218.
78. Glickman, M. H., and Klinman, J. P. (1996) Lipoxygenase reaction mechanism: Demonstration that hydrogen abstraction from substrate precedes dioxygen binding during catalytic turnover, *Biochemistry 35*, 12882−12892.
79. Knapp, M. J., and Klinman, J. P. (2003) Kinetic studies of oxygen reactivity in soybean lipoxygenase-1, *Biochemistry 42*, 11466−11475.
80. Segel, I. H. (1993) *Enzyme Kinetics: Behavior and Analysis of Rapid Equilibrium and Steady-State Systems*, pp 564−565, 324−328, Wiley, New York.
81. Tsai, A. L., Kulmacz, R. J., and Palmer, G. (1995) Spectroscopic evidence for reaction of prostaglandin H synthase-1 tyrosyl radical with arachidonic acid, *J. Biol. Chem. 270*, 10503−10508.
82. Tsai, A.-L., Palmer, G., Xiao, G., Swinney, D. C., and Kulmacz, R. J. (1998) Structural characterization of arachidonyl radicals formed by prostaglandin H synthase-2 and prostaglandin H synthase-1 reconstituted with mangano protoporphyrin IX, *J. Biol. Chem. 273*, 3888−3894.
83. Mason, R. P., Kalyanaraman, B., Tainer, B. E., and Eling, T. E. (1980) A carbon-centered free radical intermediate in the prostaglandin synthetase oxidation of arachidonic acid. Spin trapping and oxygen uptake studies, *J. Biol. Chem. 255*, 5019−5022.
84. Picot, D., Loll, P. J., and Garavito, R. M. (1994) The X-ray crystal structure of the membrane protein prostaglandin H_2 synthase-1, *Nature 367*, 243−249.
85. Pratt, D. A., Mills, J. H., and Porter, N. A. (2003) Theoretical calculations of carbon-oxygen bond dissociation enthalpies of peroxyl radicals formed in the autoxidation of lipids, *J. Am. Chem. Soc. 125*, 5801−5810.
86. Porter, N. A., and Wujek, D. G. (1984) Autoxidation of polyunsaturated fatty acids, an expanded mechanistic study, *J. Am. Chem. Soc. 106*, 2626−2629.
87. Hay, S., Westerlund, K., and Tommos, C. (2005) Moving a phenol hydroxyl group from the surface to the interior of a protein: Effects on the phenol potential and pK_A, *Biochemistry 44*, 11891−11902.
88. Li, C., and Hoffman, M. Z. (1999) One-electron redox potentials of phenols in aqueous solution, *J. Phys. Chem. B 103*, 6653−6656.
89. Glickman, M. H., and Klinman, J. P. (1995) Nature of rate-limiting steps in the soybean lipoxygenase-1 reaction, *Biochemistry 34*, 14077−14092.
90. Bhattacharyya, D. K., Lecomte, M., Rieke, C., Garavito, R. M., and Smith, W. L. (1996) Involvement of arginine 120, glutamate 524, and tyrosine 355 in the binding of arachidonate and 2-phenylpropionic acid inhibitors to the cyclooxygenase active site of ovine prostaglandin endoperoxide H synthase-1, *J. Biol. Chem. 271*, 2179−2184.

91. Furse, K. E., Pratt, D. A., Porter, N. A., and Lybrand, T. P. (2006) Molecular dynamics simulations of arachidonic acid complexes with COX-1 and COX-2: Insights into equilibrium behavior, *Biochemistry 45*, 3189−3205.
92. Laarhoven, L. J., Mulder, P., and Wayner, D. D. M. (1999) Determination of bond dissociation enthalpies in solution by photoacoustic calorimetry, *Acc. Chem. Res. 32*, 342−349.
93. Peng, S., and van der Donk, W. A. (2003) An unusual isotope effect on substrate inhibition in the oxidation of arachidonic acid by lipoxygenase, *J. Am. Chem. Soc. 125*, 8988−8989.
94. Blomberg, M. R. A., Siegbahn, P. E., Styring, S., Babcock, G. T., Åkermark, B., and Korall, P. (1997) A quantum chemical study of hydrogen abstraction from manganese-coordinated water by a tyrosyl radical: A model for water oxidation in photosystem II, *J. Am. Chem. Soc. 119*, 8285−8292.
95. Bordwell, F. G., and Cheng, J.-P. (1991) Substituent effects on the stabilities of phenoxyl radicals and the acidities of phenoxyl radical cations, *J. Am. Chem. Soc. 113*, 1736−1743.
96. Wilson, J. C., Wu, G., Tsai, A.-L., and Gerfen, G. J. (2005) Determination of the structural environment of the tyrosyl radical in prostaglandin H_2 synthase-1: A high frequency ENDOR/EPR study, *J. Am. Chem. Soc. 127*, 1618−1619.
97. Northrop, D. B. (1975) Steady-state analysis of kinetic isotope effects in enzymic reactions, *Biochemistry 14*, 2644−2651.
98. Jonsson, T., Glickman, M. H., Sun, S., and Klinman, J. P. (1996) Experimental evidence for extensive tunneling of hydrogen in the lipoxygenase reaction: Implications for enzyme catalysis, *J. Am. Chem. Soc. 118*, 10319−10320.
99. Lewis, E. R., Johansen, E., and Holman, T. R. (1999) Large competitive kinetic isotope effects in human 15-lipoxygenase catalysis measured by a novel HPLC method, *J. Am. Chem. Soc. 121*, 1395−1396.
100. Quinn, D. M., and Sutton, L. D. (1991) Theoretical basis and mechanistic utility of solvent isotope effects, in *Enzyme Mechanism from Isotope Effects* (Cook, P. F., Ed.) pp 73−126, CRC Press, Boca Raton, FL.
101. Kreevoy, M. M., and Liang, T. M. (1980) Structures and isotopic fractionation factors of complexes, *J. Am. Chem. Soc. 102*, 3315−3322.
102. Luo, M., Flamand, N., and Brock, T. G. (2006) Metabolism of arachidonic acid to eicosanoids within the nucleus, *Biochim. Biophys. Acta 1761*, 618−625.
103. Toh, H., Yokoyama, C., Tanabe, T., Yoshimoto, T., and Yamamoto, S. (1992) Molecular evolution of cyclooxygenase and lipoxygenase, *Prostaglandins 44*, 291−315.
104. Segraves, E. N., and Holman, T. R. (2003) Kinetic investigations of the rate-limiting step in human 12- and 15-lipoxygenase, *Biochemistry 42*, 5236−5243.
105. Scarrow, R. C., Trimitsis, M. G., Buck, C. P., Grove, G. N., Cowling, R. A., and Nelson, M. J. (1994) X-ray spectroscopy of the iron site in soybean lipoxygenase-1: Changes in coordination Supon oxidation or addition of methanol, *Biochemistry 33*, 15023−15035.
106. Knapp, M. J., Rickert, K., and Klinman, J. P. (2002) Temperature-dependent isotope effects in soybean lipoxygenase-1: Correlating hydrogen tunneling with protein dynamics, *J. Am. Chem. Soc. 124*, 3865−3874.
107. Roth, J. P., Yoder, J. C., Won, T.-J., and Mayer, J. M. (2001) Application of the Marcus cross relation to hydrogen atom transfer reactions, *Science 294*, 2524−2526.
108. Hatcher, E., Soudackov, A. V., and Hammes-Schiffer, S. (2004) Proton-coupled electron transfer in soybean lipoxygenase, *J. Am. Chem. Soc. 126*, 5763−5775.
109. Lingwood, M., Hammond, J. R., Hrovat, D. A., Mayer, J. M., and Borden, W. T. (2006) MPW1K performs much better than B3LYP in DFT calculations on reactions that proceed by proton-coupled electron transfer (PCET), *J. Chem. Theory Comput. 2*, 740−745.

BI602502J